## ANTHROPOLOGY

# Early human impacts and ecosystem reorganization in southern-central Africa

Jessica C. Thompson[1,2]*†, David K. Wright[3,4]*†, Sarah J. Ivory[5]*†, Jeong-Heon Choi[6], Sheila Nightingale[7], Alex Mackay[8], Flora Schilt[9,10], Erik Otárola-Castillo[11], Julio Mercader[12,13,14], Steven L. Forman[15], Timothy Pietsch[16], Andrew S. Cohen[17], J. Ramón Arrowsmith[18], Menno Welling[19,20], Jacob Davis[21], Benjamin Schiery[22], Potiphar Kaliba[23], Oris Malijani[23], Margaret W. Blome[24], Corey A. O'Driscoll[8], Susan M. Mentzer[9,25], Christopher Miller[9,26], Seoyoung Heo[6], Jungyu Choi[27], Joseph Tembo[23], Fredrick Mapemba[23], Davie Simengwa[28], Elizabeth Gomani-Chindebvu[29]

Modern *Homo sapiens* engage in substantial ecosystem modification, but it is difficult to detect the origins or early consequences of these behaviors. Archaeological, geochronological, geomorphological, and paleoenvironmental data from northern Malawi document a changing relationship between forager presence, ecosystem organization, and alluvial fan formation in the Late Pleistocene. Dense concentrations of Middle Stone Age artifacts and alluvial fan systems formed after ca. 92 thousand years ago, within a paleoecological context with no analog in the preceding half-million-year record. Archaeological data and principal coordinates analysis indicate that early anthropogenic fire relaxed seasonal constraints on ignitions, influencing vegetation composition and erosion. This operated in tandem with climate-driven changes in precipitation to culminate in an ecological transition to an early, pre-agricultural anthropogenic landscape.

## INTRODUCTION

Modern humans act as powerful agents of ecosystem transformation. They have extensively and intentionally modified their environments for tens of millennia, leading to much debate about when and how the first human-dominated ecosystems arose (*1*). A growing body of archaeological and ethnographic evidence shows substantial, recursive interactions between foragers and their environments that suggest that these behaviors were fundamental to the evolution of our species (*2*–*4*). Fossil and genetic data indicate that *Homo sapiens* were present in Africa by ~315 thousand years (ka) ago, and archaeological data show notable increases in the complexity of behavior that took place across the continent within the past ~300- to 200-ka span at the end of the Middle Pleistocene (Chibanian) (*5*). Since our emergence as a species, humans have come to rely on technological innovation, seasonal scheduling, and complex social cooperation to thrive. These attributes have enabled us to exploit previously uninhabited or extreme environments and resources, so that today humans are the only pan-global animal species (*6*). Fire has played a key role in this transformation (*7*).

Biological models suggest that adaptations for cooked food extend back at least 2 million years, but regular archaeological evidence for controlled use of fire does not appear until the end of the Middle Pleistocene (*8*). A marine core with a dust record drawn from a wide swath of the African continent shows that over the past million years, peaks in elemental carbon occurred after ~400 ka, predominantly during shifts from interglacial to glacial conditions, but also during the Holocene (*9*). This suggests that fire was less common in sub-Saharan Africa before ~400 ka and that by the Holocene, there was a substantial anthropogenic contribution (*9*). Fire is a tool that has been used by pastoralists to open and maintain grasslands throughout the Holocene (*10*). However, detecting the contexts and ecological impacts of fire use by Pleistocene early hunter-gatherers is more complex (*11*).

Fire is known both ethnographically and archaeologically as an engineering tool for resource manipulation, including improvement of subsistence returns or modification of raw materials, with these activities often associated with communal planning and requiring substantial ecological knowledge (*2*, *12*, *13*). Landscape-scale fires allow hunter-gatherers to drive game, control pests, and enhance productivity of habitat (*2*). On-site fire facilitates cooking, warmth, predator defense, and social cohesion (*14*). However, there is substantial

[1]Department of Anthropology, Yale University, New Haven, CT, USA. [2]Institute of Human Origins, P.O. Box 874101, Tempe, AZ 85287, USA. [3]Department of Archaeology, Conservation and History, University of Oslo, Oslo, Norway. [4]State Key Laboratory of Loess and Quaternary Geology, Institute of Earth Environment, Chinese Academy of Sciences, Xian, China. [5]Department of Geosciences and Earth and Environmental Systems Institute, Pennsylvania State University, University Park, PA, USA. [6]Department of Earth and Environmental Sciences, Korea Basic Science Institute, Ochang, Republic of Korea. [7]Department of Anthropology, City University of New York, Graduate Center, New York, NY, USA. [8]Centre for Archaeological Science, School of Earth, Atmospheric and Life Sciences, University of Wollongong, Wollongong, NSW, Australia. [9]Institute for Archaeological Sciences and Senckenberg Centre for Human Evolution and Palaeoenvironment, University of Tübingen, Tübingen, Germany. [10]Universidade do Algarve, Interdisciplinary Center for Archaeology and Evolution of Human Behavior (ICArEHB), FCHS, Campus Gambelas, J27, Faro 8005-139, Portugal. [11]Department of Anthropology, Purdue University, West Lafayette, IN, USA. [12]Department of Anthropology and Archaeology, University of Calgary, Calgary, AB, Canada. [13]Max Planck Institute for the Science of Human History, Jena, Germany. [14]Institut Català de Paleoecologia Humana i Evolució Social (IPHES), Zona Educacional, 4–Campus Sescelades URV (Edifici W3), 43007 Tarragona, Spain. [15]Department of Geosciences, Baylor University, Waco, TX, USA. [16]Australian Rivers Institute, Griffith University, Brisbane, QLD, Australia. [17]Department of Geosciences, University of Arizona, Tucson, AZ, USA. [18]School of Earth and Space Exploration, Arizona State University, Tempe, AZ, USA. [19]Reinwardt Academy, Amsterdam University of the Arts, Amsterdam, Netherlands. [20]African Heritage Ltd., Box 622, Zomba, Malawi. [21]Independent Researcher, New Haven, CT, USA. [22]Biostatistics Department, Medpace Inc., Cincinnati, OH, USA. [23]Malawi Department of Museums and Monuments, Lilongwe, Malawi. [24]Department of Geological Sciences, East Carolina University, Greenville, NC, USA. [25]School of Anthropology, University of Arizona, Tucson, AZ, USA. [26]SFF Centre for Early Sapiens Behaviour (SapienCE), University of Bergen, Bergen, Norway. [27]Gyeongju National Research Institute of Cultural Heritage, Gyeongju, Republic of Korea. [28]Lanjuos Social Research and Consultancy, Blantyre, Malawi. [29]Ministry of Civic Education and National Unity, Lilongwe, Malawi.
*Corresponding author. Email: jessica.thompson@yale.edu (J.C.T); david.wright@iakh.uio.no (D.K.W.); sji15@psu.edu (S.J.I.)
†These authors contributed equally to this work.

ambiguity regarding the extent to which fires by hunter-gatherers can reconfigure components of a landscape, such as ecological community structure and geomorphology (15, 16).

Understanding the development of human-induced ecological change is problematic without well-dated archaeological and geomorphic data from multiple sites, paired with continuous environmental records. Long lacustrine sedimentary records from the southern African Rift Valley, coupled with the antiquity of the archaeological record in this region, make it a place where anthropogenically induced ecological impacts may be investigated into the Pleistocene. Here, we report the archaeology and geomorphology of an extensively dated Stone Age landscape in southern-central Africa. We then link it to paleoenvironmental data spanning >600 ka to identify the earliest coupled evidence for human behavior and ecosystem transformation in the context of anthropogenic fire.

## RESULTS
### Geochronology and geomorphology
We provide previously unreported age constraints for the Chitimwe Beds of the Karonga District that lie at the northern end of Lake Malawi in the southern portion of the African Rift Valley (Fig. 1) (17). These beds are composed of lateritic alluvial fan and stream deposits that cover ~83 km$^2$, containing millions of stone artifacts, but do not have preserved organic remains such as bone (Supplementary Text) (18). Our optically stimulated luminescence (OSL) data from terrestrial records (Fig. 2 and tables S1 to S3) revise the age of the Chitimwe Beds to the Late Pleistocene, with the oldest age for both alluvial fan activation and burial of Stone Age sites ca. 92 ka (18, 19). The alluvial and fluvial Chitimwe Beds overlie Plio-Pleistocene Chiwondo Beds of lacustrine and fluvial origin in a low, angular unconformity (17). These sedimentary packages are in fault-bounded wedges along the lake margin. Their configuration indicates interactions between lake level fluctuations and active faulting extending into the Pliocene (17). Although tectonism may have affected

regional relief and piedmont slopes over an extended time, fault activity in this region likely slowed since the Middle Pleistocene (20). After ~800 ka until shortly after 100 ka, the hydrology of Lake Malawi became primarily climate driven (21). Therefore, neither is likely the sole explanation for Late Pleistocene alluvial fan formation (22).

Landscape stability after (Chitimwe) fan formation is indicated by formation of laterites and pedogenic carbonates, which cap fan deposits across the study region (Supplementary Text and table S4). The formation of alluvial fans in the Late Pleistocene of the Lake Malawi basin is not restricted to the Karonga region. About 320 km to the southeast in Mozambique, terrestrial cosmogenic nuclide depth profiles of $^{26}Al$ and $^{10}Be$ constrain formation of the alluvial, lateritic Luchamange Beds to 119 to 27 ka (23). This broad age constraint is consistent with our OSL chronology for the western Lake Malawi basin and indicates regional alluvial fan expansion in the Late Pleistocene. This is supported by data from lake core records, which suggest a higher sedimentation rate accompanied by increased terrigenous input after ca. 240 ka, with particularly high values at ca. 130 and 85 ka (Supplementary Text) (21).

### Archaeology
The earliest evidence for human occupation in the region is tied to the Chitimwe sedimentary deposits identified at ~92 ± 7 ka. This result is based on 605 m$^3$ of excavated sediment from 14 archaeological excavations with subcentimeter spatial control, and 147 m$^3$ of sediment from 46 archaeological test pits with 20-cm vertical and 2-m horizontal control (Supplementary Text and figs. S1 to S3). In addition, we have surveyed 147.5 linear km, emplaced 40 geological test pits, and analyzed over 38,000 artifacts from 60 of these localities (tables S5 and S6) (18). These extensive surveys and excavations show that while hominins, including early modern humans, may have inhabited the region before ~92 ka, depositional aggradation associated with rising and then stabilized Lake Malawi levels did not preserve archaeological evidence until formation of the Chitimwe Beds.
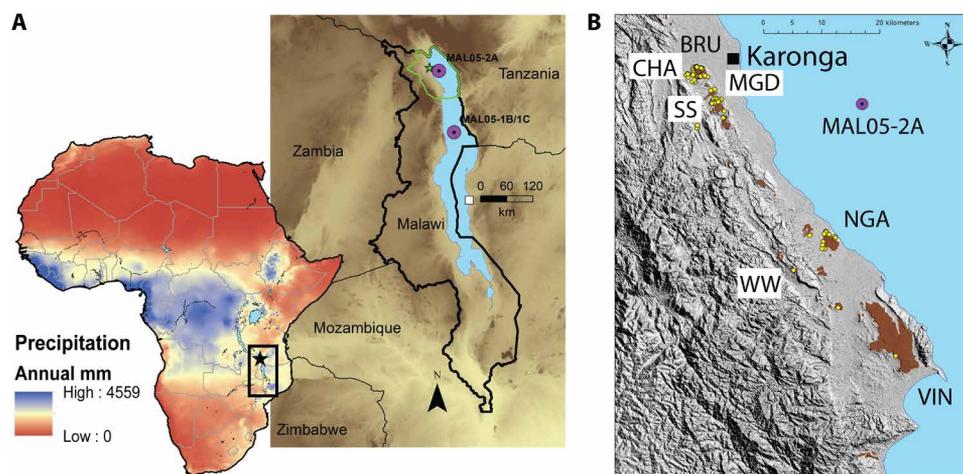


**Fig. 1. Map of region, geology, and excavation sites.** (**A**) Location of sites in Africa (star) relative to modern precipitation; blue is wetter and red is more arid (73); boxed area at left shows location of the MAL05-2A and MAL05-1B/1C cores (purple dots) in Lake Malawi and surrounding region, with the Karonga District highlighted as a green outline and location of Luchamange Beds as a white box. (**B**) Northern basin of Lake Malawi showing the hillshaded topography, remnant Chitimwe Beds (brown patches), and Malawi Earlier-Middle Stone Age Project (MEMSAP) excavation locations (yellow dots), relative to the MAL05-2A core; CHA, Chaminade; MGD, Mwanganda's Village; NGA, Ngara; SS, Sadala South; VIN, Vinthukutu; WW, White Whale.
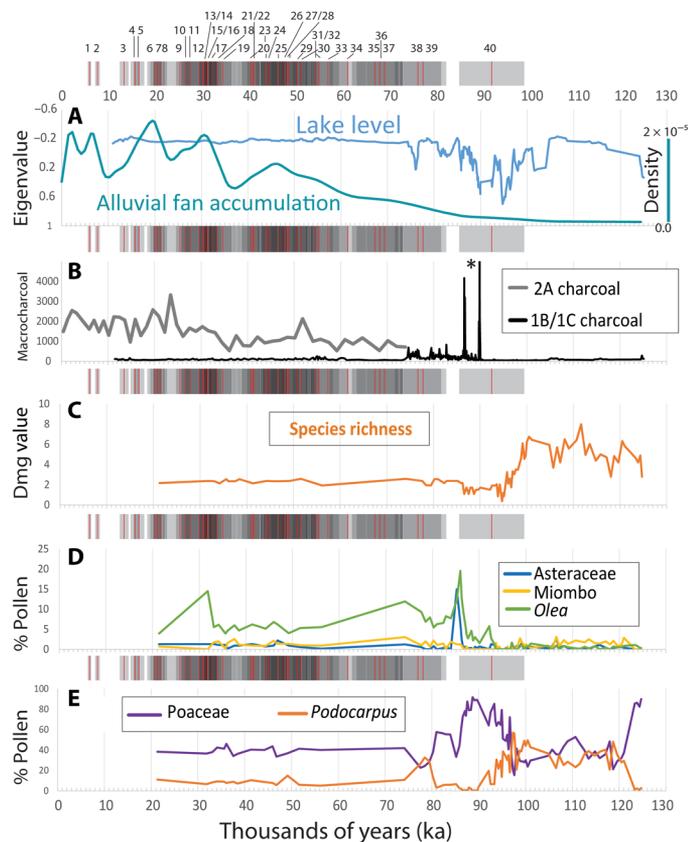
**Fig. 2. Ages of archaeological sites with geomorphic and paleoenvironmental data.** OSL central age (red lines) and error ranges at 1-σ (25% gray) for all OSL ages associated with in situ artifact occurrences in Karonga. Ages are shown against the past 125 ka of data for (**A**) Kernel density estimate of all OSL ages from alluvial fan deposits indicating sedimentation/alluvial fan accumulation (teal), and lake level reconstructions based on eigenvalues of a principal components analysis (PCA) of aquatic fossils and authigenic minerals from the MAL05-1B/1C core (*21*) (blue). (**B**) Counts of macrocharcoal per gram normalized by sedimentation rate, from the MAL05-1B/1C core (black, one value near 7000 off scale with asterisk) and MAL05-2A core (gray). (**C**) Margalef's index of species richness (Dmg) from fossil pollen of the MAL05-1B/1C core. (**D**) Percentages of fossil pollen from Asteraceae, miombo woodland, and *Olea*, and (**E**) percentages of fossil pollen from Poaceae and *Podocarpus*. All pollen data are from the MAL05-1B/1C core. Numbers at the top refer to individual OSL samples detailed in tables S1 to S3. Differences in data availability and resolution are due to different sampling intervals and material availability in the core. Figure S9 shows the two macrocharcoal records converted to *z* scores.

The archaeological data support the inference that during the Late Quaternary, fan expansion and human activities in northern Malawi were substantial, and artifacts were of a type associated elsewhere in Africa with early modern humans. The majority of artifacts were created from quartzite or quartz river cobbles and featured radial, Levallois, platform, and casual core reduction (fig. S4). Morphologically diagnostic artifacts can be predominantly attributable to Levallois-type technologies characteristic of the Middle Stone Age (MSA), known to date from at least ~315 ka in Africa (*24*). The uppermost Chitimwe Beds, which continue into the Early Holocene, contain sparsely distributed Later Stone Age occurrences, found in association with terminal Pleistocene and Holocene hunter-gatherers across Africa. In contrast, stone tool traditions typically associated with the Early and Middle Pleistocene, such as large cutting tools, are rare. Where

these do occur, they are found within MSA-bearing deposits dated to the Late Pleistocene, not an earlier phase of sedimentation (table S4) (*18*). Although sites are present from ~92 ka, the most well-represented period of both human activity and alluvial fan deposition occurs after ~70 ka, well defined by a cluster of OSL ages (Fig. 2). We confirm this pattern with 25 published and 50 previously unpublished OSL ages (Fig. 2 and tables S1 to S3). These show that of a total of 75 age determinations, 70 were recovered from sediment that postdates ~70 ka. The 40 ages associated with in situ MSA artifacts are shown in Fig. 2, relative to major paleoenvironmental indicators published from the MAL05-1B/1C central basin lake core (*25*) and previously unpublished charcoal from the MAL05-2A northern basin lake core (adjacent to the fans that produced the OSL ages).

## Paleoclimate and environment reconstruction

Climate and environmental conditions coeval with MSA human occupation at Lake Malawi were reconstructed using freshly generated data from phytoliths and soil micromorphology from archaeological excavations and published data from fossil pollen, macrocharcoal, aquatic fossils, and authigenic minerals from the Lake Malawi Drilling Project cores (*21*). The latter two proxies are the primary basis of the reconstruction of relative lake depth dating back over 1200 ka (*21*) and are matched to pollen and macrocharcoal samples taken from the same places in the core that span the past ~636 ka (*25*). The longest cores (MAL05-1B and MAL05-1C; 381 and 90 m, respectively) were collected ~100 km southeast of the archaeological project area. A shorter core (MAL05-2A; 41 m) was collected ~25 km east, offshore from the North Rukuru River (Fig. 1). The MAL05-2A core reflects terrigenous paleoenvironmental conditions of the Karonga region, whereas the MAL05-1B/1C cores did not receive direct riverine input from Karonga and thus are more reflective of regional conditions.

Sedimentation rates recorded in the MAL05-1B/1C composite drill core began to increase starting ~240 ka from a long-term average of 0.24 to 0.88 m/ka (fig. S5). The initial increase is associated with changes in orbitally modulated insolation, which drive high amplitude changes in lake level during this interval (*25*). However, when orbital eccentricity decreased and climate stabilized after 85 ka, sedimentation rates remained high (0.68 m/ka). This is concurrent with the terrestrial OSL record, which shows extensive evidence for alluvial fan expansion after ~92 ka, and congruent with magnetic susceptibility data that show a positive relationship between erosion and fire after 85 ka (Supplementary Text and table S7). Given the error ranges of available geochronological controls, it is not possible to tell whether this set of relationships evolved slowly from a progression of recursive processes or occurred in rapid bursts as tipping points were reached. On the basis of geophysical models of basin evolution, rift extension and associated subsidence have slowed since the Middle Pleistocene (*20*) and, therefore, are not the primary cause of extensive fan formation processes we have dated to mainly after 92 ka.

Climate has been the dominant control of lake level since the Middle Pleistocene (*26*). Specifically, uplift in the northern basin closed an existing outlet ca. 800 ka, allowing the lake to deepen until reaching the sill elevation of the modern outlet (*21*). This outlet, located at the southern end of the lake, provides an upper limit on lake levels during wet intervals (including the present day), but allows the basin to close as lake levels drop during periods of aridity (*27*). Lake level reconstructions show alternating wet-dry cycles over

the past 636 ka. On the basis of evidence from fossil pollen, periods of extreme aridity (>95% decrease in total water volume) linked to lows in summer insolation resulted in the expansion of semi-desert vegetation with trees restricted to permanent waterways (27). These (lake) lowstands were associated with pollen spectra showing high proportions of grass (80% or more) and xerophytic herbs (Amaranthaceae) at the expense of tree taxa and low overall species richness (25). In contrast, when the lake was near the modern level, vegetation with strong affinities to Afromontane forest typically expanded to the lakeshore [~500 m above sea level (masl)]. Today, Afromontane forests only occur in small, discontinuous patches above ~1500 masl (25, 28).

The most recent period of extreme aridity occurred from 104 to 86 ka, after which open miombo woodland with substantial grass and herbaceous components became widespread, despite recovery of the lake level to high-stand conditions (27, 28). Afromontane forest taxa, most notably *Podocarpus*, never recovered after 85 ka to values similar to previous periods of high lake levels (10.7 ± 7.6% after 85 ka versus 29.8 ± 11.8% during analogous lake level before 85 ka). Margalef's index (Dmg) also shows that the past 85 ka has been marked by species richness 43% lower than during previous sustained periods of high lake level (2.3 ± 0.20 versus 4.6 ± 1.21, respectively), for example, in the high lake period between ca. 420 and 345 ka (Supplementary Text and figs. S5 and S6) (25). Pollen samples from the period ca. 88 to 78 ka also contain high percentages of Asteraceae pollen, which can be indicative of vegetation disturbance and is within the error range of the oldest date for human occupation of the area.

## Paleoenvironmental analysis

We use a climate anomaly approach (29) to analyze paleoecological and paleoclimatic data from the drill cores before and after 85 ka and test the hypothesis that the ecological relations among vegetation, species richness, and precipitation became decoupled from predictions derived from the presumably purely climate-driven baseline pattern of the preceding ~550 ka. This transformed ecological system was influenced by both lake infilling precipitation conditions and fire occurrence, as reflected in a species-poor and novel vegetation assemblage. Only some forest elements recovered after the last arid period, and these included fire-tolerant components of the Afromontane forest such as *Olea*, and hardy components of tropical seasonal forest such as *Celtis* (Supplementary Text and fig. S5) (25). To test this hypothesis, we model lake level derived from ostracode and authigenic mineral proxies as the independent variable (21) versus dependent variables such as charcoal and pollen that could have been affected by increased fire frequency (25).

To examine how similar or dissimilar the assemblages were to one another at different times, we conducted a principal coordinates analysis (PCoA) using pollen from *Podocarpus* (evergreen tree), Poaceae (grasses), *Olea* (a fire-tolerant component of Afromontane forest), and miombo (the dominant woodland component today). By mapping the PCoA on top of an interpolated surface that represents lake level at the time each assemblage was formed, we examine how pollen assemblages changed relative to precipitation and how this relationship changed after 85 ka (Fig. 3 and fig. S7). Before 85 ka, samples dominated by Poaceae cluster toward drier conditions, while samples dominated by *Podocarpus* cluster toward wetter conditions. In contrast, samples dating to after 85 ka cluster away from the majority of pre-85-ka samples and have a different average value,
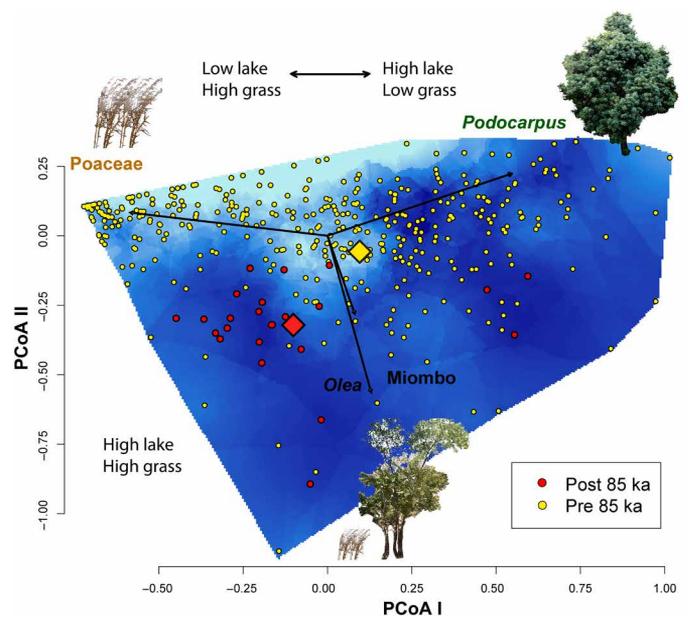


**Fig. 3. PCoA analysis of pollen from Lake Malawi core MAL05-1B/1C (25).** Each dot represents a single pollen sample at a given point in time, using the age model in the Supplementary Text and fig. S8. Vectors show the direction and gradient of change, with longer vectors representing a stronger trend. The underlying surface represents lake levels as a proxy for precipitation; darker blue is higher. A mean value for the PCoA eigenvalues is provided for the post-85-ka data (red diamond) and all pre-85-ka data from analogous lake levels (yellow diamond). "Analogous lake levels" are between −0.130-σ and −0.198-σ around the mean eigenvalue of the lake level PCA using the entire 636 ka of data.

showing that their composition is unusual for similar precipitation conditions. Their position in the PCoA reflects the influence of *Olea* and miombo, both of which are favored under more fire-prone conditions. Of the post-85-ka samples, *Podocarpus* is only abundant in three successive samples, which occurred just after the onset of this interval between 78 and 79 ka. This suggests that after initial rainfall increase, forests appear to make a brief recovery before eventual collapse.

To investigate the relations among the pollen, lake levels, and charcoal, we used a nonparametric multivariate analysis of variance (NP-MANOVA) to compare the total "environment" (represented by a data matrix of pollen, lake levels, and charcoal), before and after the transition at 85 ka. We found that variation and covariation found in this data matrix are statistically significantly different before and after 85 ka (Table 1).

Our terrestrial paleoenvironmental data from phytoliths and soils on the western lake margins agree with interpretations based on proxies from the lake. These show that despite high lake levels, the landscape had transitioned to one dominated by open canopy woodland and wooded grassland, much as today (25). All localities analyzed for phytoliths on the western margin of the basin date to after ~45 ka and show substantial arboreal cover that reflect wet conditions. However, they suggest that much of that cover is in the form of open woodlands in cohort with bambusoid and panicoid grasses. On the basis of phytolith data, fire-intolerant palms (Arecaceae) were present exclusively by the lake shoreline and rare or absent from inland archaeological sites (table S8) (30).

In general, wet but open conditions in the later part of the Pleistocene are also inferred from terrestrial paleosols (19). Lagoonal clay and

**Table 1. Results of MANOVA using *Podocarpus*, Poaceae, *Olea*, miombo, charcoal, and lake level as proxies for the environment.** DF, degrees of freedom.

| | DF | SumSquares | MeanSquares | F. model | $R^2$ | Pr (>F) |
|---|---|---|---|---|---|---|
| Age > 85 ka | 1 | 3.337 | 3.3374 | 13.603 | 0.0326 | <0.0001 |
| Residuals | 404 | 99.121 | 0.2453 | | 0.9674 | |
| Total | 405 | 102.458 | | | 1.0000 | |

palustrine-pedogenic carbonates from the vicinity of the Mwanganda's Village archaeological site date between 40 and 28 cal ka BP (calibrated kiloanni before present) (table S4). Carbonate soil horizons within the Chitimwe Beds are typically nodular calcretes (Bkm) and argillic and carbonate (Btk) horizons, which indicate locations of relative landform stability with slow sedimentation derived from distal alluvial fan progradation by ca. 29 cal ka BP (Supplementary Text). Eroded, indurated laterite soils (petroplinthites) formed on remnants of paleofans are indicative of open landscape conditions (*31*) with strongly seasonal precipitation (*32*), illustrating the ongoing legacy of these conditions on the landscape.

Support for the role of fire in this transformation comes from the paired macrocharcoal records from the drill cores, which from the central basin (MAL05-1B/1C) show an overall increase in charcoal influx starting ca. 175 ka. Substantial peaks follow between ca. 135 and 175 ka and 85 and 100 ka, after which time lake levels recover but forest trees and species richness do not (Supplementary Text, Fig. 2, and fig. S5). The relationship between charcoal influx and magnetic susceptibility of lake sediments can also show patterns in long-term fire history (*33*). Using data from Lyons *et al.* (*34*), ongoing erosion of burned landscapes after 85 ka is implied at Lake Malawi by a positive correlation (Spearman's $R$s = 0.2542 and $P$ = 0.0002; table S7), whereas older sediments show an inverse relationship ($R$s = −0.2509 and $P$ < 0.0001). In the northern basin, the shorter MAL05-2A core has its deepest chronological anchor point with the Youngest Toba Tuff at ~74 to 75 ka (*35*). Although it lacks the longer-term perspective, it receives input directly from the catchment from which the archaeological data derive. The north basin charcoal record shows a steady increase in terrigenous charcoal input since the Toba crypto-tephra marker, over the period where archaeological evidence is most prevalent (Fig. 2B).

## DISCUSSION

Evidence for anthropogenic fire may reflect intentional use at the landscape scale, widespread populations creating more or larger on-site ignitions, alteration of fuel availability through harvesting of the understory, or a combination of these activities. Modern hunter-gatherers use fire to actively modify foraging returns (*2*). Their activities increase prey abundances, maintain mosaic landscapes, and increase pyrodiversity and succession stage heterogeneity (*13*). Fire is also important for on-site activities such as heat, cooking, defense, and socialization (*14*). Even small differences in the deployment of fire outside of natural lightning strikes can alter patterns of forest succession, fuel availability, and seasonality of ignitions. Reductions in arboreal cover and woody understory have the most potential to enhance erosion, while loss of species diversity in this region is tightly tied to loss of Afromontane forest communities (*25*).

Human control of fire is well established in the archaeological record from before the start of the MSA (*15*), but its use as a landscape management tool has only so far been documented in a few Paleolithic contexts. These include in Australia ca. 40 ka (*36*), Highland New Guinea ca. 45 ka (*37*), and ca. 50 ka at Niah Cave in lowland Borneo (*38*). In the Americas, anthropogenic ignitions have been implicated as major factors in the reconfiguration of faunal and floral communities as humans first entered these ecosystems, especially within the past 20 ka (*16*). These conclusions are necessarily based on correlative evidence, but the argument for a cause-and-effect relationship is strengthened where there is direct overlap of archaeological, geochronological, geomorphic, and paleoenvironmental data. Although marine core data offshore of Africa have previously provided evidence of altered fire regimes over the past ~400 ka (*9*), here, we provide evidence of anthropogenic impacts that draw from correlated archaeological, paleoenvironmental, and geomorphic datasets.

Identifying anthropogenic fire in the paleoenvironmental record requires evidence of temporal or spatial changes in fire activity and vegetation, demonstration that these changes are not predicted by climate parameters alone, and temporal/spatial coincidence between fire regime changes and changes in the human record (*29*). Here, the first evidence for extensive MSA occupation and alluvial fan formation in the Lake Malawi basin occurred alongside a major reorganization of regional vegetation that began ca. 85 ka. Charcoal abundances in the MAL05-1B/1C core are reflective of regional trends in charcoal production and sedimentation that show substantial differences after ca. 150 ka when compared to the rest of the 636-ka record (figs. S5, S9, and S10). This transition shows an important contribution of fire for shaping ecosystem composition that cannot be explained by climate alone. In natural fire regimes, lightning ignitions typically occur at the end of the dry season (*39*). Anthropogenic fires, however, may be ignited at any time if fuels are sufficiently dry. On a site scale, humans can alter fire regimes continuously through collection of firewood from the understory. The net result of anthropogenic fire of any kind is that it has the potential to result in more consumption of woody vegetation, continuously throughout the year, and at a variety of scales.

In South Africa, fire was used in the heat treatment of stone for tool manufacture as early as 164 ka (*12*) and as a tool for cooking starchy tubers as early as 170 ka (*40*), taking advantage of resources that thrived in ancient fire-prone landscapes (*41*). Landscape fires reduce arboreal cover and are crucial tools in maintaining grassland and forest patch environments, which are defining elements of anthropogenically mediated ecosystems (*13*). If modification of vegetation or prey behavior was the intent of increased anthropogenic burning, then this behavior represents an increase in the complexity with which early modern humans controlled and deployed fire in comparison to earlier hominins and shows a transformed interdependency in our relationship with fire (*7*). Our analysis offers an additional

avenue for understanding how human use of fire changed in the Late Pleistocene and what impacts these changes had on their landscapes and environments.

The expansion of alluvial fans during the Late Quaternary in the Karonga region may be attributable to changes in seasonal burning cycles under higher-than-average rainfall conditions, which resulted in enhanced hillslope erosion. The mechanism through which this occurred was likely by driving watershed-scale responses from fire-induced disturbance with enhanced and sustained denudation in the upper portions of the watersheds, and alluvial fan expansion in the piedmont environments adjacent to Lake Malawi. These responses likely included changes in soil properties to decrease infiltration rates, diminished surface roughness, and enhanced runoff as high precipitation conditions combined with reduced arboreal cover (42). Sediment availability is enhanced initially by the stripping of cover material and over longer time scales potentially by loss of soil strength from heating and from decreased root strength. The stripping of topsoil increased sediment flux, which was accommodated by fan aggradation downstream and accelerated laterite formation on the fans.

Many factors can control the landscape response to changing fire regime, and most of them operate at short time scales (42–44). The signal we associate here is manifest at the thousand-year time scale. Analytical and landscape evolution models have shown notable denudation rate changes over thousand-year time scales with recurrent wildfire-induced vegetation disturbances (45, 46). A lack of regional fossil records contemporaneous with the observed changes in charcoal and vegetation records impedes reconstruction of the impacts of human behavior and environmental change on herbivore community composition. However, large grazing herbivores that inhabit landscapes that are more open play a role in maintaining them and in keeping woody vegetation from encroaching (47). Evidence of change across different components of the environment should not be expected to be simultaneous, but rather viewed as a series of cumulative effects that may have occurred over a prolonged period (11). Using a climate anomaly approach (29), we attribute human activity as a key driver in shaping the landscape of northern Malawi over the course of the Late Pleistocene. However, these impacts may be built on an earlier, less visible legacy of human-environment interactions. Charcoal peaks that appear in the paleoenvironmental record before the earliest archaeological dates may include an anthropogenic component that did not result in the same ecological regime change that is documented later in time and that did not involve sedimentation sufficient to confidently indicate human occupation.

Short sediment cores, such as that from the adjacent Lake Masoko basin in Tanzania, or shorter cores within Lake Malawi itself, show changes in the relative pollen abundances of grass to woodland taxa that have been attributed to natural climate variability over the past 45 ka (48–50). However, it is only with the longer perspective of the >600-ka pollen record of Lake Malawi, accompanied by the extensively dated archaeological landscape next to it, that it is possible to understand the longer-term associations between climate, vegetation, charcoal, and human activity. Although humans were likely present in the northern Lake Malawi basin before 85 ka, the density of archaeological sites after ca. 85 ka, and especially after 70 ka, indicates that the region was attractive for human occupation after the last major arid period ended. At this time, novel or more intensive/frequent usage of fire by humans

apparently combined with natural climate shifts to restructure a >550-ka ecological relationship, ultimately generating an early preagricultural anthropogenic landscape (Fig. 4). Unlike during earlier time periods, the depositional nature of this landscape preserved MSA sites as a function of the recursive relationship between environment (resource distributions), human behavior (activity patterns), and fan activation (sedimentation/site burial).

The Anthropocene represents the accumulation of niche construction behaviors that have developed over millennia, at a scale unique to modern *H. sapiens* (1, 51). In the modern context, anthropogenic landscapes persist and have intensified following the introduction of agriculture, but they are extensions, not disconnections, of patterns established during the Pleistocene (52). Data from northern Malawi show that periods of ecological transition can be prolonged, complex, and iterative. Transformations of this scale reflect complex ecological knowledge by early modern humans
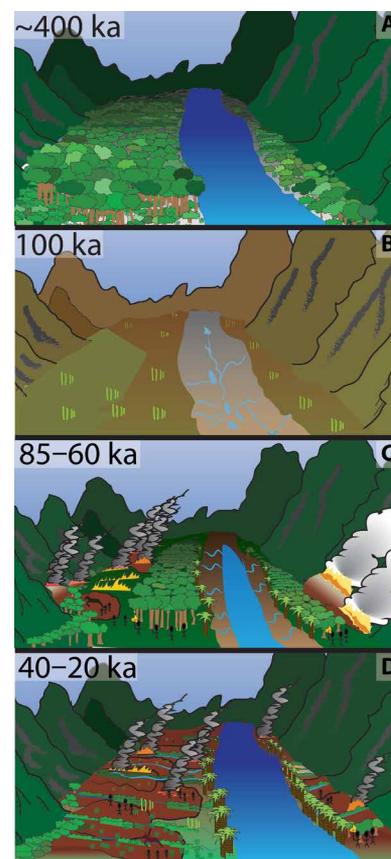


**Fig. 4. Landscape evolution and ecology of the northern Lake Malawi basin.** (**A**) ca. 400 ka: No detectable human presence. Wet conditions similar to today with high lake level. Diverse, non–fire-tolerant arboreal cover. (**B**) ca. 100 ka: No archaeological record, but human presence possibly detected by charcoal influx. Extremely arid conditions occur in a desiccated watershed. Commonly exposed bedrock, limited surface sediment. (**C**) ca. 85 to 60 ka: Lake level is increasing with higher precipitation. Human presence archaeologically detectable after 92 ka and concentrated after 70 ka. Burning of uplands and alluvial fan expansion ensue. Less diverse, fire-tolerant vegetation regime emerges. (**D**) ca. 40 to 20 ka: Ambient charcoal input in the northern basin increases. Alluvial fan formation continues but begins to abate toward the end of this period. Lake levels remain high and stable relative to the preceding 636-ka record.

and illustrate their transition to the globally dominant species we are today.

## MATERIALS AND METHODS
### Fieldwork survey, excavation, and profile documentation
Site survey and recording of artifact and cobble characteristics on survey tracts followed protocols described in Thompson *et al.* (*53*). Test pit emplacement and main site excavation, including micromorphology and phytolith sampling, followed protocols described in Thompson *et al.* (*18*) and Wright *et al.* (*19*). Our Geographic Information System (GIS) maps based on Malawi geological survey maps of the region show a clear association between the Chitimwe Beds and archaeological sites (fig. S1). Placement of geologic and archaeological test pits in the Karonga region was spaced to capture the broadest representative sample possible (fig. S2). Geomorphic, geochronometric, and archaeological investigations of Karonga involved four main field approaches: pedestrian survey, archaeological test pitting, geological test pitting, and detailed site excavations. Together, these techniques allowed major exposures of the Chitimwe Beds to be sampled in the northern, central, and southern parts of Karonga (fig. S3).

Site survey and recording of artifact and cobble characteristics on pedestrian survey tracts followed protocols described in Thompson *et al.* (*53*). This approach had two main goals. The first was to identify localities where artifacts were actively eroding, and then place archaeological test pits upslope at those localities to recover artifacts in situ from buried contexts. The second goal was to formally document the distribution of artifacts, their characteristics, and their relationship to nearby sources of lithic raw material (*53*). For this work, a crew comprising three people walked at 2- to 3-m spacing for a combined total of 147.5 linear km, transecting across most of the mapped Chitimwe Beds (table S6).

Work concentrated first on the Chitimwe Beds to maximize the sample of observed artifacts, and second on long linear transects from the lakeshore to the uplands that crosscut different sedimentary units. This confirmed the key observation that artifacts located between the western highlands and the lakeshore are exclusively associated with the Chitimwe Beds or more recent Late Pleistocene and Holocene deposits. Artifacts found in other deposits are ex situ and have been relocated from elsewhere on the landscape, as revealed by their abundances, sizes, and degree of weathering.

Archaeological test pit emplacement and main site excavation, including micromorphology and phytolith sampling, followed protocols described in Thompson *et al.* (*18*, *54*) and Wright *et al.* (*19*, *55*). The primary aim was to understand the subsurface distribution of artifacts and fan deposits across the larger landscape. Artifacts are typically deeply buried within the Chitimwe Beds in all places except at the margins, where erosion has begun to remove the top part of the deposit. During informal survey, two people walked across Chitimwe Beds that appear as mapped features on Government of Malawi geological maps. As these people encountered the shoulders of Chitimwe Bed deposits, they began to walk along the margins where they could observe artifacts eroding from the deposits. By placing excavations slightly (3 to 8 m) upslope from actively eroding artifacts, excavations could reveal their in situ locations relative to their containing sediments, without the necessity of laterally extensive excavations. Test pits were emplaced so that they would be 200- to 300-m distant from the next-nearest pit and thus capture the variation across Chitimwe Bed deposits and the artifacts they contained. In some cases, test pits revealed localities that later became the sites of full excavations.

All test pits began as 1 × 2 m squares, oriented north-south, and excavated in 20-cm arbitrary units, unless there was a noticeable change in sediment color, texture, or inclusions. Sedimentologic and pedologic attributes were recorded for all excavated sediment, which was passed uniformly through a 5-mm dry sieve. If deposit depth continued beyond 0.8 to 1 m, then excavation ceased in one of the two square meters and continued in the other, thus creating a "step" so that the deeper layers could be safely accessed. Excavation then continued until bedrock was reached, at least 40 cm of archaeologically sterile sediment had been reached below a concentration of artifacts, or excavation became too unsafe (deep) to proceed. In some cases, deposit depth required extension of the test pit into a third square meter, with two steps into the trench.

Geologic test pits had previously revealed that the Chitimwe Beds often appear on geologic maps because of a distinctive reddish color, when they include a wide range of stream and river deposits, alluvial fan deposits, and do not always present as red in color (*19*). Geologic test pits were excavated as simple pits designed to clean off mixed upper sediments to reveal the subsurface stratigraphy of deposits. This was necessary because the Chitimwe Beds erode as parabolic hillslopes with slumped sediments coating the slope and do not typically form clear natural sections or cuts. These excavations thus occurred either at the tops of Chitimwe Beds, where there was an inferred subsurface contact between the Chitimwe Beds and the underlying Pliocene Chiwondo Beds, or where river terrace deposits required dating (*55*).

Full archaeological excavations proceeded at localities that promised large assemblages of in situ stone artifacts, typically based on test pits or where artifacts could be seen eroding in large quantities from a slope. Artifacts from the main excavations were recovered from sedimentary units that were excavated separately in 1 × 1 m squares. Units were excavated as spits of either 10 or 5 cm if artifact densities were high. All stone artifacts, fossil bone, and ochre were piece plotted at each main excavation, with no size cutoff. The sieve size was 5 mm. Artifacts were assigned unique barcoded plotted find numbers if they were recovered during excavation, and find numbers within the same series were assigned to sieved finds. Artifacts were labeled with permanent ink, placed in a bag with their specimen label, and bagged together with other artifacts from the same context. After analysis, all artifacts were stored at the Cultural and Museum Centre, Karonga.

All excavation was conducted according to natural layers. These were subdivided into spits, with spit thickness dependent on artifact density (e.g., spit thickness would be high if artifact density was low). Context data (e.g., sediment attributes, context relationships, and observations about disturbances and artifact densities) were recorded in an Access database. All coordinate data (e.g., piece-plotted finds, context elevations, square corners, and samples) are based on Universal Transverse Mercator (UTM) coordinates (WGS 1984, Zone 36S). At main sites, all points were recorded using a Nikon Nivo C-series 5″ total station that was established within a local grid oriented as closely as possible to UTM north. The location of the northwest corner of each excavated site and the volume of sediment removed for each are given in table S5.

Profiles of sedimentologic and pedologic features were documented from all excavation units using the U.S. Department of Agriculture classification scheme (*56*). Sedimentologic units were designated on the basis of grain sizes, angularity, and bedding features. Anomalous inclusions and disturbances relative to the

sediment unit were noted. Soil development was determined on the basis of subsurface accumulation of sesquioxides or carbonates in the subsoils. Subaerial weathering (e.g., redox, residual Mn nodule formation) was also commonly documented.

## OSL dating

Collection points for OSL samples were determined on the basis of an estimation of which facies were likely to yield the most reliable estimation of sediment burial age. At sample locations, trenches were made to expose authigenic sediment layers. All samples for OSL dating were collected by inserting light-tight steel tubes (approximately 4 cm in diameter and 25 cm in length) into the sediment profiles.

OSL dating measures the size of the population of trapped electrons within crystals such as quartz or feldspar arising from exposure to ionizing radiation. The bulk of this radiation originates from the decay of radioactive isotopes within the environment with a minor additional component in the tropical latitudes coming in the form of cosmic radiation. Trapped electrons are released upon exposure of the crystals to light, which occurs either during transport (the zeroing event) or in the laboratory, where illumination occurs beneath a sensor (for example, a photomuliplier tube or charged couple device camera) that can detect photons emitted when the electrons return to their ground state. Quartz grains measuring between 150 and 250 μm were isolated through sieving, acid treatments and density separations, and analyzed either as small aliquots (<100 grains) mounted to the surface of aluminum disks or as single grains held within 300 by 300 mm wells drilled into an aluminum disc. Burial doses were typically estimated using single aliquot regeneration methods (57). In addition to assessment of the radiation dose received by grains, OSL dating also requires estimation of the dose rate through measurements using gamma spectrometry or neutron activation analysis of radionuclide concentrations within the sediments from which the sample was collected, along with determination of a cosmic dose rate by reference to the sample location and burial depth. Final age determination is achieved by dividing the burial dose by the dose rate. However, statistical modeling is required to determine an appropriate burial dose to use when there is a variation in the doses measured for individual grains or groups of grains. Burial doses were calculated here using the Central Age Model, in the case of single aliquot dating, or the finite mixture model in the case of single grain dating (58).

Three separate laboratories performed OSL analysis for this study. Detailed individual methods for each laboratory are presented below. In general, we applied OSL dating using regenerative-dose methods to small aliquots (tens of grains) rather than using single grain analysis. This is because small aliquots of samples had low recuperation ratios (<2%) during regenerative growth experiments and the OSL signals were not saturated at the levels of natural signals. Interlaboratory consistency of age determinations, consistent harmony of results within and between stratigraphic sections tested, and parity with geomorphic interpretations of ^{14}C ages from carbonates were the primary basis of this assessment. Single grain protocols were evaluated or performed at each laboratory, but independently determined to be inappropriate for use in this study. Detailed methods and analytical protocols followed by individual laboratories are provided in Supplementary Materials and Methods.

## Lithic analysis

Lithic artifacts recovered from controlled excavations (BRU-I; CHA-I, CHA-II, and CHA-III; MGD-I, MGD-II, and MGD-III; and SS-I)

were analyzed and described according to metric and qualitative characteristics. Weight and maximum dimension were measured for each artifact (weight was measured to 0.1 g using a digital scale; all dimensions measured to 0.01 mm with Mitutoyo digital calipers). All artifacts were also classified according to raw material (quartz, quartzite, chert, and other), grain size (fine, medium, and coarse), grain size homogeneity, color, cortex type and coverage, weathering/edge rounding, and technological class (complete or fragmentary core or flake, flake piece/angular shatter, hammerstone, manuport, and other).

Cores were measured along their maximum length; maximum width; width at 15, 50, and 85% of length; maximum thickness; and thickness at 15, 50, and 85% of length. Measurements were also taken to assess the volumetric attributes of hemispherically organized (radial and Levallois) cores. Both complete and broken cores were classified according to reduction method (single or multiplatform, radial, Levallois, and other), and flake scars were counted at both ≥15 mm and at ≥20% of core length. Cores with five or fewer scars 15 mm were classified as "casual." Cortex coverage was recorded for the total core surface, and on hemispherically organized cores, the relative cortex coverage was recorded for each side.

Flakes were measured along their maximum length; maximum width; width at 15, 50, and 85% of length; maximum thickness; and thickness at 15, 50, and 85% of length. Fragmentary flakes were described according to the portion preserved (proximal, medial, distal, split right, and split left). Elongation was calculated by dividing maximum length by maximum width. Platform width, thickness, and exterior platform angle were measured on complete flakes and proximal flake fragments, and platforms were classified according to degree of preparation. Cortex coverage and location were recorded on all flakes and fragments. Distal edges were classified according to termination type (feather, hinge, and overshot). On complete flakes, the number and orientation of prior flake scars were recorded. When encountered, retouch location and invasiveness were recorded following the protocol established by Clarkson (59). Refitting programs were initiated for most of the excavated assemblages to assess reduction methods and site depositional integrity.

Lithic artifacts recovered from test pits (CS-TP1-21, SS-TP1-16, and NGA-TP1-8) were described according to a simpler scheme than those from controlled excavations. For each artifact, the following characteristics were recorded: raw material, grain size, cortex coverage, size class, weathering/edge damage, technological component, and preserved portion of fragmentary pieces. Descriptive notes were recorded for diagnostic features of flakes and cores.

## Micromorphology and carbonate dating

Intact blocks of sediment were cut from profiles exposed in excavations and geological trenches. These blocks were stabilized in the field, using either plaster-of-Paris bandages or toilet paper and packaging tape, and transported to the Geoarchaeology Laboratory at the University of Tübingen, Germany. There, the samples were dried at 40°C for at least 24 hours. They were then indurated under vacuum, using a mixture of unpromoted polyester resin and styrene at a ratio of 7:3. Methyethylketone peroxide was used as the catalyst, with resin-styrene mixture (3 to 5 ml/liter). Once the resin mixture had gelled, the samples were heated at 40°C for at least 24 hours to completely harden the mixture. The hardened samples were cut with a tile saw into chips measuring 6 × 9 cm, which were glued to a glass slide and ground to a thickness of 30 μm. The resulting thin

sections were scanned using a flatbed scanner and analyzed under the naked eye and under magnification (×50 to ×200) using plane-polarized light, cross-polarized light, oblique incident light, and blue-light fluorescence. Terminology and descriptions of the thin sections follow guidelines published by Stoops (60) and Courty et al. (61). Pedogenic carbonate nodules, collected from a depth of >80 cm, were sliced in half so that one half could be impregnated and studied in thin section (4.5 × 2.6 cm), using standard stereoscopic and petrographic microscopes, as well as cathodoluminescence (CL) microscopy. Control on the type of carbonate was given much care, as pedogenic carbonates form in connection to a stable ground surface, while groundwater carbonates form independently from a ground surface or soil.

Samples were drilled from the cut faces of pedogenic carbonate nodules, which were halved to be used for various analyses. The thin sections were studied by F.S. with standard stereo and petrographic microscopes of the working group for geoarchaeology and with a CL microscope at the working group for experimental mineralogy, both in Tübingen, Germany. Subsamples for radiocarbon dating were drilled with a precision drill from designated areas of ca. 3 mm in diameter in the opposing half of the nodule, avoiding zones with late recrystallization, abundant mineral inclusions, or great variability in calcite crystal sizes. The same protocol could not be followed for samples MEM-5038, MEM-5035, and MEM-5055 A, which were selected from loose sediment samples and too small to be cut in half for thin sectioning. However, corresponding micromorphological samples of the adjacent sediment, including carbonate nodules, were studied in thin section.

We submitted samples for $^{14}$C dating to the Center for Applied Isotope Studies (CAIS), at the University of Georgia, Athens, USA. The carbonate samples were reacted with 100% phosphoric acid in evacuated reaction vessels to produce $CO_2$. $CO_2$ samples were cryogenically purified from the other reaction products and catalytically converted to graphite. Graphite $^{14}$C/$^{13}$C ratios were measured using a 0.5-MeV accelerator mass spectrometer. The sample ratios were compared to the ratio measured from the oxalic acid I standard (NBS SRM 4990). Carrara marble (IAEA C1) was used as the background, and travertine (IAEA C2) was used as a secondary standard. The results are presented as percent modern carbon, and the quoted uncalibrated dates are given in radiocarbon years before 1950 (years BP), using the $^{14}$C half-life of 5568 years. The error is quoted as 1-σ and reflects both statistical and experimental errors. The dates have been corrected for isotope fractionation based on the isotope-ratio mass spectrometry–measured δ$^{13}$C values reported by C. Wissing at the laboratory for Biogeology in Tübingen, Germany, except in the case of UGAMS-35944r, which was measured at CAIS. Sample 6887B was analyzed in duplicate. A second subsample was drilled from the nodule for this purpose (UGAMS-35944r) from the sampling region indicated on the cut surface. All samples were corrected for atmospheric fractionation of $^{14}$C to 2-σ using the southern hemisphere application of the INTCAL20 calibration curve (table S4) (62).

## Phytolith analysis

Sample (sediment, 0.7 g) was mixed with 0.1% preboiled solution of sodium hexametaphosphate $Na_6[(PO_3)_6]$ and sonicated (5 min). Orbital shaking took place overnight at 200 rpm. After clay dispersal, 3 N hydrochloric and nitric acids (HCl) (HNO$_3$) plus hydrogen peroxide (H$_2$O$_2$) were added. Then, sodium polytungstate (3Na$_2$WO$_4$·9WO$_3$·H$_2$O)

(Poly-Gee) at specific gravity 2.4 (preboiled) separated out phytoliths. This was followed by rinsing and centrifugation of samples at 3000 rpm for 5 min. Aliquots (15 μl) were mounted on boiled microscope slides with Entellan New (cover, 20 × 40 mm = inspected area). System microscopy was performed at 40× (Olympus BX41, Motic BA410E). Classification nomenclature followed the International Code for Phytolith Nomenclature (63). The referential baseline included modern plants from several African ecoregions (64) and local soils (65), as well as archaeological localities in the Malawi basin (19, 66).

## Statistical methods

The OSL data from the landscape and paleoecological data from the Lake Malawi 1B/1C core were subjected to statistical analyses to examine how they changed before and after ~85 ka. Kernel density estimates (KDEs) of sedimentation were constructed following protocols developed in Vermeesch (67) and Kappler et al. (68) from 72 luminescence ages interpreted as originating from alluvial fan deposits (tables S1 to S3). KDEs provide reliable distributions of age occurrences when standard errors (SEs) overlap or the analytical imprecision of the true age is high (67). For the present analysis, each age was replotted 10,000 times along a normal distribution using the rnorm command in R based on the laboratory generated mean and 1-σ SE. The KDE was created in the "kde1d" package in R (69). Bandwidth was set to default, with data-derived parameters developed by Sheather and Jones (70).

To characterize the biotic environment, we used proportions of pollen from Poaceae, Podocarpus, miombo, and Olea. We used lake levels to characterize the abiotic environment. Over the ~636 ka span of the MAL05-1B/1C core for which pollen data are available, there have been several periods when lake level was equivalent to modern conditions. We have defined these analogous conditions by downsampling the published lake level data (21) to fit the pollen sample intervals (25), and then calculating the statistical mean of the principal components analysis (PCA) eigenvalue for all lake level proxies over the past 74 ka to represent "modern-like" lake conditions. The pollen sampling intervals effectively make this the statistical mean of lake levels between 21.4 and 56.2 ka [−0.130-σ and −0.198-σ (25)] and enable us to compare recent vegetation composition to its composition during older, analogous precipitation regimes.

To evaluate whether there were differences in the regional environmental structure before and after 85 ka, we conducted a NP-MANOVA (71). However, vegetation and lake level proxies are inherently different data types [pollen proportions (25) and the first principal component of all lake level proxies (21), respectively]. To conduct the MANOVA, these data must be the same type. Pollen, lake level proxies, and macrocharcoal were also sampled at different densities and intervals in the cores. To properly adjust the data so that once a single pollen sample and its age are matched to a single charcoal and lake level sample, we conducted a series of transformations. Because the pollen data were the most sparsely sampled, we used a spline to fit and downsample the lake level and charcoal data to match them. To make the pollen and lake level data equivalent, we conducted a PCoA using R software (72). PCoA is similar to the widely known PCA in that PCoA conducts a decomposition of a data matrix to obtain eigenvalues and their corresponding eigenvectors. The difference is that while PCA decomposes the variance-covariance matrix, PCoA solves for the eigenvalues of a distance matrix of the original data. To create the distance matrix, we used

the $\chi^2$ distance, which is appropriate for proportion data, like pollen. The PCoA results in a set of scores, representing the original data, which can be plotted similar to PCA. In our case, these scores are not only useful for graphic illustration, but as they are normalized and Euclidean, they are identical to the lake level data and maintain all information contained by the original pollen dataset. This procedure allowed us to use the PCoA pollen scores in conjunction with lake level variable in the NP-MANOVA to test whether there was a difference in environment before and after 85 ka. For the Supplementary Materials statistics, biplots of species richness and lake level were constructed using the "ggplot2" package of R. Box and whiskers quartiles used the "boxplot" command in base R.

## SUPPLEMENTARY MATERIALS

Supplementary material for this article is available at http://advances.sciencemag.org/cgi/content/full/7/19/eabf9776/DC1

## REFERENCES AND NOTES

1. N. L. Boivin, M. A. Zeder, D. Q. Fuller, A. Crowther, G. Larson, J. M. Erlandson, T. Denham, M. D. Petraglia, Ecological consequences of human niche construction: Examining long-term anthropogenic shaping of global species distributions. *Proc. Natl. Acad. Sci. U.S.A.* **113**, 6388–6396 (2016).
2. F. Scherjon, C. Bakels, K. MacDonald, W. Roebroeks, Burning the land: An ethnographic study of off-site fire use by current and historically documented foragers and implications for the interpretation of past fire practices in the landscape. *Curr. Anthropol.* **56**, 299–326 (2015).
3. S. White, Grass páramo as hunter-gatherer landscape. *Holocene* **23**, 898–915 (2013).
4. R. Bliege Bird, C. McGuire, D. W. Bird, M. H. Price, D. Zeanah, D. G. Nimmo, Fire mosaics and habitat choice in nomadic foragers. *Proc. Natl. Acad. Sci. U.S.A.* **117**, 12904–12914 (2020).
5. E. M. L. Scerri, M. G. Thomas, A. Manica, P. Gunz, J. T. Stock, C. Stringer, M. Grove, H. S. Groucutt, A. Timmermann, G. P. Rightmire, F. d'Errico, C. A. Tryon, N. A. Drake, A. S. Brooks, R. W. Dennell, R. Durbin, B. M. Henn, J. Lee-Thorp, P. deMenocal, M. D. Petraglia, J. C. Thompson, A. Scally, L. Chikhi, Did our species evolve in subdivided populations across Africa, and why does it matter? *Trends Ecol. Evol.* **33**, 582–594 (2018).
6. P. Roberts, B. A. Stewart, Defining the 'generalist specialist' niche for Pleistocene *Homo sapiens*. *Nat. Hum. Behav.* **2**, 542–550 (2018).
7. R. Biggs, W. Boonstra, G. Peterson, M. Schlüter, The domestication of fire as a social-ecological regime shift. *PAGES—Past Global Chang. Mag.* **24**, 22–23 (2016).
8. J. A. J. Gowlett, The discovery of fire by humans: A long and convoluted process. *Philos. Trans. R. Soc. Lond. B Biol. Sci.* **371**, 20150164 (2016).
9. M. I. Bird, J. A. Cali, A million-year record of fire in sub-Saharan Africa. *Nature* **394**, 767–769 (1998).
10. C. W. Marean, Implications of late Quaternary mammalian fauna from Lukenya Hill (south-central Kenya) for paleoenvironmental change and faunal extinctions. *Quatern. Res.* **37**, 239–255 (1992).
11. J. C. Thompson, D. K. Wright, S. J. Ivory, The emergence and intensification of early hunter-gatherer niche construction. *Evol. Anthropol.* **30**, 17–27 (2021).
12. K. S. Brown, C. W. Marean, A. I. R. Herries, Z. Jacobs, C. Tribolo, D. Braun, D. L. Roberts, M. C. Meyer, J. Bernatchez, Fire as an engineering tool of early modern humans. *Science* **325**, 859–862 (2009).
13. R. Bliege Bird, D. W. Bird, L. E. Fernandez, N. Taylor, W. Taylor, D. Nimmo, Aboriginal burning promotes fine-scale pyrodiversity and native predators in Australia's Western Desert. *Biol. Conserv.* **219**, 110–118 (2018).
14. P. W. Wiessner, Embers of society: Firelight talk among the Ju/'hoansi Bushmen. *Proc. Natl. Acad. Sci.* **111**, 14027–14035 (2014).
15. A. Glikson, Fire and human evolution: The deep-time blueprints of the Anthropocene. *Anthropocene* **3**, 89–92 (2013).
16. N. Pinter, S. Fiedel, J. E. Keeley, Fire and vegetation shifts in the Americas at the vanguard of Paleoindian migration. *Quat. Sci. Rev.* **30**, 269–272 (2011).
17. U. Ring, C. Betzler, Geology of the Malawi Rift: Kinematic and tectonosedimentary background to the Chiwondo Beds, northern Malawi. *J. Hum. Evol.* **28**, 7–21 (1995).
18. J. C. Thompson, A. Mackay, S. Nightingale, D. Wright, J. H. Choi, M. Welling, H. Blackmore, E. Gomani-Chindebvu, Ecological risk, demography and technological complexity in the Late Pleistocene of northern Malawi: Implications for geographical patterning in the Middle Stone Age. *J. Quat. Sci.* **33**, 261–284 (2018).
19. D. K. Wright, J. C. Thompson, F. Schilt, A. S. Cohen, J.H. Choi, J. Mercader, S. Nightingale, C. E. Miller, S. M. Mentzer, D. Walde, M. Welling, E. Gomani-Chindebvu, Approaches

20. E. Mortimer, D. A. Paton, C. A. Scholz, M. R. Strecker, P. Blisniuk, Orthogonal to oblique rifting: Effect of rift basin orientation in the evolution of the North basin, Malawi Rift, East Africa. *Basin Res.* **19**, 393–407 (2007).
21. S. J. Ivory, M. W. Blome, J. W. King, M. M. McGlue, J. E. Cole, A. S. Cohen, Environmental change explains cichlid adaptive radiation at Lake Malawi over the past 1.2 million years. *Proc. Natl. Acad. Sci. U.S.A.* **113**, 11895–11900 (2016).
22. D. Delvaux, *Peri-Tethys Memoir: PeriTethyan Rift/Wrench Basins and Passive Margins,* P. A. Ziegler, W. Cavazza, A. H. F. Robertson, S. Crasquin-Soleau, Eds. (Memoirs of the National Museum of Natural History, Paris 2001), pp. 545–567.
23. J. Mercader, J. C. Gosse, T. Bennett, A. J. Hidy, D. H. Rood, Cosmogenic nuclide age constraints on Middle Stone Age lithics from Niassa, Mozambique. *Quat. Sci. Rev.* **47**, 116–130 (2012).
24. D. Richter, R. Grün, R. Joannes-Boyau, T. E. Steele, F. Amani, M. Rué, P. Fernandes, J. P. Raynal, D. Geraads, A. Ben-Ncer, J. J. Hublin, S. P. McPherron, The age of the hominin fossils from Jebel Irhoud, Morocco, and the origins of the Middle Stone Age. *Nature* **546**, 293–296 (2017).
25. S. J. Ivory, A.-M. Lézine, A. Vincens, A. Cohen, Waxing and waning of forests: Late Quaternary biogeography of southeast Africa. *Glob. Chang. Biol.* **24**, 2939–2951 (2018).
26. C. A. Scholz, T. C. Johnson, A. S. Cohen, J. W. King, J. A. Peck, J. T. Overpeck, M. R. Talbot, E. T. Brown, L. Kalindekafe, P. Y. O. Amoako, R. P. Lyons, T. M. Shanahan, I. S. Castaneda, C. W. Heil, S. L. Forman, L. R. McHargue, K. R. Beuning, J. Gomez, J. Pierson, East African megadroughts between 135 and 75 thousand years ago and bearing on early-modern human origins. *Proc. Natl. Acad. Sci. U.S.A.* **104**, 16416–16421 (2007).
27. R. P. Lyons, C. A. Scholz, A. S. Cohen, J. W. King, E. T. Brown, S. J. Ivory, T. C. Johnson, A. L. Deino, P. N. Reinthal, M. M. McGlue, M. W. Blome, Continuous 1.3-million-year record of East African hydroclimate, and implications for patterns of evolution and biodiversity. *Proc. Natl. Acad. Sci. U.S.A.* **112**, 15568–15573 (2015).
28. S. J. Ivory, R. Early, D. F. Sax, J. Russell, Niche expansion and temperature sensitivity of tropical African montane forests. *Glob. Ecol. Biogeogr.* **25**, 693–703 (2016).
29. D. M. J. S. Bowman, J. Balch, P. Artaxo, W. J. Bond, M. A. Cochrane, C. M. D'Antonio, R. Defries, F. H. Johnston, J. E. Keeley, M. A. Krawchuk, C. A. Kull, M. Mack, M. A. Moritz, S. Pyne, C. I. Roos, A. C. Scott, N. S. Sodhi, T. W. Swetnam, R. Whittaker, The human dimension of fire regimes on Earth. *J. Biogeogr.* **38**, 2223–2236 (2011).
30. J. Mercader, F. Astudillo, M. Barkworth, T. Bennett, C. Esselmont, R. Kinyanjui, D. L. Grossman, S. Simpson, D. Walde, Poaceae phytoliths from the Niassa Rift, Mozambique. *J. Archaeol. Sci.* **37**, 1953–1967 (2010).
31. N. van Breemen, P. Buurman, *Soil Formation,* N. van Breemen, P. Buurman, Eds. (Springer Netherlands, Dordrecht, 1998), pp. 291–312.
32. B. P. Finney, T. C. Johnson, Sedimentation in Lake Malawi (East Africa) during the past 10,000 years: A continuous paleoclimatic record from the southern tropics. *Palaeogeogr. Palaeoclimatol. Palaeoecol.* **85**, 351–366 (1991).
33. C. Whitlock, C. Larsen, Charcoal as a fire proxy, in *Tracking Environmental Change Using Lake Sediments: Terrestrial, Algal, and Siliceous Indicators,* J. P. Smol, H. J. B. Birks, W. M. Last, R. S. Bradley, K. Alverson, Eds. (Springer Netherlands, 2001), pp. 75–97.
34. R. P. Lyons, C. A. Scholz, M. R. Buoniconti, M. R. Martin, Late Quaternary stratigraphic analysis of the Lake Malawi Rift, East Africa: An integration of drill-core and seismic-reflection data. *Palaeogeogr. Palaeoclimatol. Palaeoecol.* **303**, 20–37 (2011).
35. C. L. Yost, L. J. Jackson, J. R. Stone, A. S. Cohen, Subdecadal phytolith and charcoal records from Lake Malawi, East Africa imply minimal effects on human evolution from the ~74 ka Toba supereruption. *J. Hum. Evol.* **116**, 75–94 (2018).
36. S. van der Kaars, G. H. Miller, C. S. M. Turney, E. J. Cook, D. Nürnberg, J. Schönfeld, A. P. Kershaw, S. J. Lehman, Humans rather than climate the primary cause of Pleistocene megafaunal extinction in Australia. *Nat. Commun.* **8**, 14142 (2017).
37. G. R. Summerhayes, M. Leavesley, A. Fairbairn, H. Mandui, J. Field, A. Ford, R. Fullagar, Human adaptation and plant use in highland New Guinea 49,000 to 44,000 years ago. *Science* **330**, 78–81 (2010).
38. C. O. Hunt, D. D. Gilbertson, G. Rushworth, A 50,000-year record of late Pleistocene tropical vegetation and human impact in lowland Borneo. *Quat. Sci. Rev.* **37**, 61–80 (2012).
39. Y. Le Page, D. Oom, J. M. N. Silva, P. Jönsson, J. M. C. Pereira, Seasonality of vegetation fires as modified by human action: Observing the deviation from eco-climatic fire regimes. *Glob. Ecol. Biogeogr.* **19**, 575–588 (2010).
40. L. Wadley, L. Backwell, F. d'Errico, C. Sievers, Cooked starchy rhizomes in Africa 170 thousand years ago. *Science* **367**, 87–91 (2020).
41. T. Kraaij, F. Engelbrecht, J. Franklin, R. M. Cowling, A fiery past: A comparison of glacial and contemporary fire regimes on the Palaeo-Agulhas Plain, Cape Floristic Region. *Quat. Sci. Rev.* **235**, 106059 (2020).
42. J. A. Moody, R. A. Shakesby, P. R. Robichaud, S. H. Cannon, D. A. Martin, Current research issues related to post-wildfire runoff and erosion processes. *Earth Sci. Rev.* **122**, 10–37 (2013).
43. R. A. DiBiase, M. P. Lamb, Vegetation and wildfire controls on sediment yield in bedrock landscapes. *Geophys. Res. Lett.* **40**, 1093–1097 (2013).

44. S. J. Ivory, M. M. McGlue, G. S. Ellis, A. M. Lézine, A. S. Cohen, A. Vincens, Vegetation controls on weathering intensity during the last deglacial transition in Southeast Africa. *PLOS ONE* **9**, e112855 (2014).

45. E. Istanbulluoglu, R. L. Bras, Vegetation-modulated landscape evolution: Effects of vegetation on landscape processes, drainage density, and topography. *J. Geophys. Res. Earth* **110**, F02012 (2005).

46. C. A. Orem, J. D. Pelletier, The predominance of post-wildfire erosion in the long-term denudation of the Valles Caldera, New Mexico. *J. Geophys. Res. Earth* **121**, 843–864 (2016).

47. I. P. J. Smit, H. H. T. Prins, Predicting the effects of woody encroachment on mammal communities, grazing biomass and fire frequency in African savannas. *PLOS ONE* **10**, e0137857 (2015).

48. Y. Garcin, A. Vincens, D. Williamson, G. Buchet, J. Guiot, Abrupt resumption of the African Monsoon at the Younger Dryas—Holocene climatic transition. *Quat. Sci. Rev.* **26**, 690–704 (2007).

49. S. J. Ivory, A.-M. Lézine, A. Vincens, A. S. Cohen, Effect of aridity and rainfall seasonality on vegetation in the southern tropics of East Africa during the Pleistocene/Holocene transition. *Quatern. Res.* **77**, 77–86 (2012).

50. G. H. DeBusk, A 37,500-year pollen record from Lake Malawi and implications for the biogeography of afromontane forests. *J. Biogeogr.* **25**, 479–500 (1998).

51. E. C. Ellis, Anthropogenic transformation of the terrestrial biosphere. *Philos. Trans. R. Soc. A Math. Phys. Eng. Sci.* **369**, 1010–1035 (2011).

52. A. M. Bauer, E. C. Ellis, The anthropocene divide: Obscuring understanding of social-environmental change. *Curr. Anthropol.* **59**, 209–227 (2018).

53. J. C. Thompson, A. Mackay, V. de Moor, E. Gomani-Chindebvu, Catchment survey in the Karonga District: A landscape-scale analysis of Provisioning and core reduction strategies during the Middle Stone Age of northern Malawi. *African Archaeol. Rev.* **31**, 447–478 (2014).

54. J. C. Thompson, A. Mackay, D. K. Wright, M. Welling, A. Greaves, E. Gomani-Chindebvu, D. Simengwa, Renewed investigations into the Middle Stone Age of northern Malawi. *Quatern. Int.* **270**, 129–139 (2012).

55. D. K. Wright, J. Thompson, A. Mackay, M. Welling, S. L. Forman, G. Price, J. X. Zhao, A. S. Cohen, O. Malijani, E. Gomani-Chindebvu, Renewed geoarchaeological investigations of Mwanganda's Village (Elephant Butchery Site), Karonga, Malawi. *Geoarchaeology* **29**, 98–120 (2014).

56. P. J. Schoeneberger, D. A. Wysocki, E. C. Benham; Soil Survey Staff, *Field Book for Describing and Sampling Soils, Version 3.0* (Natural Resources Conservation Service, National Soil Survey Center, 2012).

57. A. S. Murray, A. G. Wintle, The single aliquot regenerative dose protocol: Potential for improvements in reliability. *Radiat. Meas.* **37**, 377–381 (2003).

58. R. F. Galbraith, R. G. Roberts, Statistical aspects of equivalent dose and error calculation and display in OSL dating: An overview and some recommendations. *Quat. Geochronol.* **11**, 1–27 (2012).

59. C. Clarkson, An index of invasiveness for the measurement of unifacial and bifacial retouch: A theoretical, experimental and archaeological verification. *J. Archaeol. Sci.* **29**, 65–75 (2002).

60. G. Stoops, *Guidelines for Analysis and Description of Soil and Regolith Thin Sections* (Soil Science Society of America, Inc., 2003).

61. M. A. Courty, P. Goldberg, R. Macphail, *Soils and Micromorphology in Archaeology* (Cambridge Manuals in Archaeology, Cambridge Univ. Press, 1989).

62. A. G. Hogg, T. J. Heaton, Q. Hua, J. G. Palmer, C. S. M. Turney, J. Southon, A. Bayliss, P. G. Blackwell, C. B. Ramsey, C. Pearson, F. Petchey, P. Reimer, R. Reimer, L. Wacker, SHCal20 southern hemisphere calibration, 0–55,000 years Cal BP. *Radiocarbon*, 759–778 (2020).

63. M. Madella, A. Alexandré, T. Ball, International code for phytolith nomenclature 1.0. *Ann. Bot.* **96**, 253–260 (2005).

64. F. Runge, The opal phytolith inventory of soils in central Africa—Quantities, shapes, classification, and spectra. *Rev. Palaeobotany Palynol.* **107**, 23–53 (1999).

65. J. Mercader, T. Bennett, C. Esselmont, S. Simpson, D. Walde, Soil phytoliths from miombo woodlands in Mozambique. *Quatern. Res.* **75**, 138–150 (2011).

66. J. Mercader, T. Bennett, C. Esselmont, S. Simpson, D. Walde, Phytoliths from Middle Stone Age habitats in the Mozambican Rift (105-29 ka). *J. Hum. Evol.* **64**, 328–336 (2013).

67. P. Vermeesch, On the visualisation of detrital age distributions. *Chem. Geol.* **312-313**, 190–194 (2012).

68. C. Kappler, K. Kaiser, M. Küster, A. Nicolay, A. Fülling, O. Bens, T. Raab, Late Pleistocene and Holocene terrestrial geomorphodynamics and soil formation in northeastern Germany: A review of geochronological data. *Phys. Geogr.* **40**, 405–432 (2019).

69. G. Geenens, C. Wang, Local-likelihood transformation Kernel Density Estimation for positive random variables. *J. Comput. Graph. Stat.* **27**, 822–835 (2018).

70. S. J. Sheather, M. C. Jones, A reliable data-based bandwidth selection method for Kernel Density Estimation. *J. R. Stat. Soc. B. Methodol.* **53**, 683–690 (1991).

71. E. Otárola-Castillo, M. G. Torquato, H. C. Hawkins, E. James, J. A. Harris, C. W. Marean, S. P. McPherron, J. C. Thompson, Differentiating between cutting actions on bone using 3D geometric morphometrics and Bayesian analyses with implications to human evolution. *J. Archaeol. Sci.* **89**, 56–67 (2018).

72. R Core Team, *R: A Language and Environment for Statistical Computing* (R Foundation for Statistical Computing, 2020).

73. R. J. Hijmans, S. E. Cameron, J. L. Parra, P. G. Jones, A. Jarvis, Very high resolution interpolated climate surfaces for global land areas. *Int. J. Climatol.* **25**, 1965–1978 (2005).

74. A. S. Murray, A. G. Wintle, Luminescence dating of quartz using an improved single-aliquot regenerative-dose protocol. *Radiat. Meas.* **32**, 57–73 (2000).

75. A. G. Wintle, A. S. Murray, A review of quartz optically stimulated luminescence characteristics and their relevance in single-aliquot regeneration dating protocols. *Radiat. Meas.* **41**, 369–391 (2006).

76. R. F. Galbraith, R. G. Roberts, G. M. Laslett, H. Yoshida, J. M. Olley, Optical dating of single and multiple grains of quartz from Jinmium Rock Shelter, Northern Australia: Part I, Experimental design and statistical models. *Archaeometry* **41**, 339–364 (1999).

77. J. M. Olley, A. Murray, R. G. Roberts, The effects of disequilibria in the uranium and thorium decay chains on burial dose rates in fluvial sediments. *Quat. Sci. Rev.* **15**, 751–760 (1996).

78. D. W. Zimmerman, Thermoluminescent dating using fine grains from pottery. *Archaeometry* **13**, 29–52 (1971).

79. J. R. Prescott, J. T. Hutton, Cosmic ray contributions to dose rates for luminescence and ESR dating: Large depths and long-term time variations. *Radiat. Meas.* **23**, 497–500 (1994).

80. V. Mejdahl, H. H. Christiansen, Procedures used for luminescence dating of sediments. *Quat. Sci. Rev.* **13**, 403–406 (1994).

81. L. Bøtter-Jensen, E. Bulur, G. A. T. Duller, A. S. Murray, Advances in luminescence instrument systems. *Radiat. Meas.* **32**, 523–528 (2000).

82. L. J. Arnold, R. G. Roberts, Stochastic modelling of multi-grain equivalent dose (De) distributions: Implications for OSL dating of sediment mixtures. *Quat. Geochronol.* **4**, 204–230 (2009).

83. A. C. Londoño, S. L. Forman, T. Eichler, J. Pierson, Episodic eolian deposition in the past ca. 50,000years in the Alto Ilo dune field, southern Peru. *Palaeogeogr. Palaeoclimatol. Palaeoecol.* **346-347**, 12–24 (2012).

84. J. Fain, S. Soumana, M. Montret, D. Miallier, T. Pilleyre, S. Sanzelle, Luminescence and ESR dating beta-dose attenuation for various grain shapes calculated by a Monte-Carlo method. *Quat. Sci. Rev.* **18**, 231–234 (1999).

85. W. R. Van Schumus, Natural radioactivity in crust and mantle, in *Global Earth Physics: A Handbook of Physical Constants,* T. J. Ahrens, Ed. (American Geophysical Union, 1995), pp. 283–291.

86. M. J. Aitken, *An Introduction to Optical Dating: The Dating of Quaternary Sediments by the Use of Photon-Stimulated Luminescence* (Oxford Univ. Press, 1998).

87. J. M. Olley, T. Pietsch, R. G. Roberts, Optical dating of Holocene sediments from a variety of geomorphic settings using single grains of quartz. *Geomorphology* **60**, 337–358 (2004).

88. R. G. Roberts, R. F. Galbraith, H. Yoshida, G. M. Laslett, J. M. Olley, Distinguishing dose populations in sediment mixtures: A test of single-grain optical dating procedures using mixtures of laboratory-dosed quartz. *Radiat. Meas.* **32**, 459–465 (2000).

89. S. Stokes, S. Ingram, M. J. Aitken, F. Sirocko, R. Anderson, D. Leuschner, Alternative chronologies for Late Quaternary (Last Interglacial–Holocene) deep sea sediments via optical dating of silt-sized quartz. *Quat. Sci. Rev.* **22**, 925–941 (2003).

90. V. Mejdahl, Thermoluminescence dating: Beta-dose attenuation in quartz grains. *Archaeometry* **21**, 61–72 (1997).

91. M. Jain, L. Bøtter-Jensen, A. Singhvi, Dose evaluation using multiple-aliquot quartz OSL: Test of methods and a new protocol for improved accuracy and precision. *Radiat. Meas.* **37**, 67–80 (2003).

92. J. D. Clark, C. V. Haynes Jr., An elephant butchery site at Mwanganda's Village, Karonga, Malawi, and its relevance for Palaeolithic archaeology. *World Archaeol.* **1**, 390–411 (1970).

93. C. B. Ramsey, M. Scott, J. van der Plicht, Calibration for archaeological and environmental terrestrial samples in the time range 26–50 ka cal BP. *Radiocarbon* **55**, 2021–2027 (2013).

94. C. Betzler, U. Ring, Sedimentology of the Malawi Rift: Facies and stratigraphy of the Chiwondo Beds, northern Malawi. *J. Hum. Evol.* **28**, 23–35 (1995).

95. F. Dixey, The Tertiary and post-Tertiary lacustrine sediments of the Nyasan Rift-Valley. *Quat. J. Geol. Soc. Lond.* **83**, 432–442 (1927).

96. A. M. Alonso-Zarza, V. P. Wright, Calcretes, in *Carbonates in Continental Settings: Facies, Environments and Processes, Developments in Sedimentology,* A. M. Alonso-Zarza, L. H. Tanner, Eds. (Elsevier, 2010), vol. 61, pp. 225–267.

97. G. M. Ashley, D. M. Deocampo, J. Kahmann-Robinson, S. G. Driese, Groundwater-fed wetland sediments and paleosols: It's all about water table, in *New Frontiers In Paleopedology And Terrestrial Paleoclimatology*, S. G. Driese, L. C. Nordt, Eds. (SEPM Society for Sedimentary Geology, 2013), vol. 104, pp. 47–61.

98. K. Zamanian, K. Pustovoytov, Y. Kuzyakov, Pedogenic carbonates: Forms and formation processes. *Earth Sci. Rev.* **157**, 1–17 (2016).

99. M. N. Machette, Calcic Soils of the Southwestern United States, in *Soils and Quaternary Geology of the Southwestern United States: Geological Society of America Special Paper,* D. L. Weide, M. L. Faber, Eds. (Geological Society of America, 1985), vol. 203, pp. 1–21.

100. Z. Naiman, J. Quade, P. J. Patchett, Isotopic evidence for eolian recycling of pedogenic carbonate and variations in carbonate dust sources throughout the southwest United States. *Geochim. Cosmochim. Acta* **64**, 3099–3109 (2000).

101. J. Quade, A. R. Chivas, M. T. McCulloch, Strontium and carbon isotope tracers and the origins of soil carbonate in South Australia and Victoria. *Palaeogeogr. Palaeoclimatol. Palaeoecol.* **113**, 103–117 (1995).

102. C. V. Haynes, Interim report on the Quaternary geology of northern Malawi and southern Tanzania. *Quaternaria* **13**, 307–318 (1970).

103. Z. M. Kaufulu, Sedimentary environments at the Mwanganda site, Malawi. *Geoarchaeology* **5**, 15–27 (1990).

104. E. A. Stephens, Geological account of the northwest coast of Lake Malawi between Karonga and Lion Point, Malawi. *Am. Anthrop.* **68**, 50–58 (1966).

105. A. M. Alonso-Zarza, V. P. Wright, Palustrine carbonates, in *Carbonates in Continental Settings: Facies, Environments and Processes, Developments in Sedimentology* A. M. Alonso-Zarza, L. H. Tanner, Eds. (Elsevier, 2010), vol. 61, pp. 103–131.

106. P. Freytet, E. P. Verrecchia, Lacustrine and palustrine carbonate petrography: An overview. *J. Paleolimnol.* **27**, 221–237 (2002).

107. A. S. Goudie, Calcrete, in *Chemical Sediments and Geomorphology,* A. S. Goudie, K. Pye, Eds. (Academic Press, 1983), pp. 93–131.

108. E. P. Verrecchia, Litho-diagenetic implications of the calcium oxalate-carbonate biogeochemical cycle in semiarid Calcretes, Nazareth, Israel. *Geomicrobiol. J.* **8**, 87–99 (1990).

109. R. Amit, Biogenic calcic horizon development under extremely arid conditions, Nizzana Sand Dunes, Israel. *Adv. GeoEcol.* **28**, 65–88 (1995).

110. R. J. Schaetzl, S. Anderson, *Soil Genesis and Geomorphology* (Cambridge Univ. Press, 2005).

111. J. L. Slate, G. A. Smith, Y. Wang, T. E. Cerling, Carbonate-paleosol genesis in the Plio-Pleistocene St. David Formation, southeastern Arizona. *J. Sediment. Res.* **66**, 85–94 (1996).

112. V. P. Wright, Calcrete, in *Geochemical Sediments and Landscapes,* D. J. Nash, S. J. McLaren, Eds. (Blackwell Publishing, 2007), pp. 10–45.

113. P. Alonso, C. Dorronsoro, J. A. Egido, Carbonatation in palaeosols formed on terraces of the Tormes river basin (Salamanca, Spain). *Geoderma* **118**, 261–276 (2004).

114. G. Taylor, R. A. Eggleton, *Regolith Geology and Geomorphology* (John Wiley & Sons, Chicester, 2001).

115. V. P. Wright, *Soil Micromorphology: A Basic and Applied Science,* L. A. Douglas, Ed. (Elsevier, 1990), pp. 401–407.

116. G. Cailleau, E. P. Verrecchia, O. Braissant, L. Emmanuel, The biogenic origin of needle fibre calcite. *Sedimentology* **56**, 1858–1875 (2009).

117. E. P. Verrecchia, K. E. Verrecchia, Needle-fiber calcite; A critical review and a proposed classification. *J. Sediment. Res.* **64**, 650–664 (1994).

118. M. Wieder, D. H. Yaalon, Micromorphological fabrics and developmental stages of carbonate nodular forms related to soil characteristics. *Geoderma* **28**, 203–220 (1982).

119. R. Crossley, Controls of sedimentation in the Malawi rift valley, Central Africa. *Sediment. Geol.* **40**, 33–50 (1984).

120. J. R. Stone, K. S. Westover, A. S. Cohen, Late Pleistocene paleohydrography and diatom paleoecology of the central basin of Lake Malawi, Africa. *Palaeogeogr. Palaeoclimatol. Palaeoecol.* **303**, 51–70 (2011).

121. M. J. Vepraskas, L. P. Wilding, L. R. Drees, Aquic conditions for Soil Taxonomy: Concepts, soil morphology and micromorphology, in *Developments in Soil Science,* A. J. Ringrose-Voase, G. S. Humphreys, Eds. (Elsevier, 1993), vol. 22, pp. 117–131.

122. M. J. McFarlane, *Laterite and Landscape* (Academic Press, 1976).

123. M. J. McFarlane, Mechanisms for lateritisation and the formation of erosion surfaces in parts of east and southern Africa. *Bulletin de la Société Géographique de Liège* **27**, 149–155 (1991).

124. S. Nightingale, F. Schilt, J. C. Thompson, D. K. Wright, S. Forman, J. Mercader, P. Moss, S. Clarke, M. Itambu, E. Gomani-Chindebvu, M. Welling, Late Middle Stone age behavior and environments at chaminade I (Karonga, Malawi). *J. Paleolithic Archaeol.* **2**, 258–297 (2019).

125. J. E. Delvigne, *Atlas of Micromorphology of Mineral Alteration and Weathering* (Mineralogical Association of Canada, 1998).

126. I. Kovda, A. R. Mermut, Vertic features, in *Interpretation of Micromorphological Features of Soils and Regoliths,* G. Stoops, V. Marcelino, F. Mees, Eds. (Elsevier, 2010), pp. 109–127.

127. C. A. Stiles, C. I. Mora, S. G. Driese, Pedogenic iron-manganese nodules in Vertisols: A new proxy for paleoprecipitation? *Geology* **29**, 943–946 (2001).

128. M. J. McFarlane, D. J. Bowden, Mobilization of aluminium in the wathering profiles of the African surface in Malawi. *Earth Surf. Process. Landf.* **17**, 789–805 (1992).

129. E. Fritsch, C. R. Montes-Lauar, R. Boulet, A. J. Melfi, E. Balan, P. Magat, Lateritic and redoximorphic features in a faulted landscape near Manaus, Brazil. *Eur. J. Soil Sci.* **53**, 203–217 (2002).

130. Y. Tardy, *Petrology of Laterites and Tropical Soils* (A. A. Balkema Publishers, 1997).

131. S. H. Ambrose, Chronology of the Later Stone Age and food production in East Africa. *J. Archaeol. Sci.* **25**, 377–392 (1998).

132. K. Douze, A. Delagnes, The pattern of emergence of a Middle Stone Age tradition at Gademotta and Kulkuletti (Ethiopia) through convergent tool and point technologies. *J. Hum. Evol.* **91**, 93–121 (2016).

133. S. McBrearty, A. S. Brooks, The revolution that wasn't: A new interpretation of the origin of modern human behavior. *J. Hum. Evol.* **39**, 453–563 (2000).

134. C. R. Johnson, S. McBrearty, 500,000 year old blades from the Kapthurin Formation, Kenya. *J. Hum. Evol.* **58**, 193–200 (2010).

135. J. Wilkins, M. Chazan, Blade production ~500 thousand years ago at Kathu Pan 1, South Africa: Support for a multiple origins hypothesis for early Middle Pleistocene blade technologies. *J. Archaeol. Sci.* **39**, 1883–1900 (2012).

136. E. M. Scerri, J. Blinkhorn, K. Niang, M. D. Bateman, H. S. Groucutt, Persistence of Middle Stone Age technology to the Pleistocene/Holocene transition supports a complex hominin evolutionary scenario in West Africa. *J. Archaeol. Sci. Rep.* **11**, 639–646 (2017).

137. C. Tribolo, A. Asrat, J. J. Bahain, C. Chapon, E. Douville, C. Fragnol, M. Hernandez, E. Hovers, A. Leplongeon, L. Martin, D. Pleurdeau, O. Pearson, S. Puaud, Z. Assefa, Across the gap: Geochronological and sedimentological analyses from the Late Pleistocene-Holocene sequence of Goda Buticha, Southeastern Ethiopia. *PLOS ONE* **12**, e0169418 (2017).

138. A. J. H. Goodwin, An introduction to the Middle Stone Age in South Africa. *S. Afr. J. Sci.* **25**, 410–418 (1928).

139. A. J. H. Goodwin, C. Van Riet Lowe, The Stone Age cultures of South Africa. *Ann. S. Afr. Mus.* **27**, 1–289 (1929).

140. J. D. Clark, C. V. Haynes, J. E. Mawby, A. Gautier, Preliminary investigations in Malawi. *Quaternaria*, 305–354 (1970).

141. K. Faegri, J. Iversen, P. E. Kaland, K. Krzywinski, *Textbook of Pollen Analysis* (Blackburn Press, ed. 4th, 1989).

142. J. Maley, Contributions a l'etude du Bassin tchadien Atlas de pollens du Tchad. *Bull. Jard. Bot. Nat. Belg.* **40**, 29–48 (1970).

143. R. Bonnefille, G. Riollet, *Pollens de Savanes d'Afrique Orientale* (Éditions du Centre national de la recherche scientifique, Paris, 1980).

144. E. C. Grimm, *Tilia and Tiliagraph* (Illinois State Museum, 1991).

145. E. C. Grimm, CONISS: A FORTRAN 77 program for stratigraphically constrained cluster analysis by the method of incremental sum of squares. *Comput. Geosci.* **13**, 13–35 (1987).

146. R. Margalef, Information theory in ecology. *Int. J. Gen. Syst.* **3**, 36–71 (1958).

147. J. Mercader, T. Bennett, C. Esselmont, S. Simpson, D. Walde, Phytoliths in woody plants from the miombo woodlands of Mozambique. *Ann. Bot.* **104**, 91–113 (2009).

148. R. M. Albert, M. K. Bamford, D. Cabanes, Taphonomy of phytoliths and macroplants in different soils from Olduvai Gorge (Tanzania) and the application to Plio-Pleistocene palaeoanthropological samples. *Quatern. Int.* **148**, 78–94 (2006).

149. B. M. Campbell, *The Miombo in transition: Woodlands and welfare in Africa* (Bogor, Indonesia, Center for International Forestry Research, 1996).

150. C. M. Ryan, M. Williams, How does fire intensity and frequency affect miombo woodland tree populations and biomass? *Ecol. Appl.* **21**, 48–60 (2011).

151. W. A. Hoffmann, E. L. Geiger, S. G. Gotsch, D. R. Rossatto, L. C. R. Silva, O. L. Lau, M. Haridasan, A. C. Franco, Ecological thresholds at the savanna-forest boundary: How plant traits, resources and fire govern the distribution of tropical biomes. *Ecol. Lett.* **15**, 759–768 (2012).

152. C. A. Scholz, A. S. Cohen, T. C. Johnson, J. King, M. R. Talbot, E. T. Brown, Scientific drilling in the Great Rift Valley: The 2005 Lake Malawi Scientific Drilling Project—An overview of the past 145,000 years of climate variability in Southern Hemisphere East Africa. *Palaeogeogr. Palaeoclimatol. Palaeoecol.* **303**, 3–19 (2011).

153. J. Jouzel, V. Masson-Delmotte, O. Cattani, G. Dreyfus, S. Falourd, G. Hoffmann, B. Minster, J. Nouet, J. M. Barnola, J. Chappellaz, H. Fischer, J. C. Gallet, S. Johnsen, M. Leuenberger, L. Loulergue, D. Luethi, H. Oerter, F. Parrenin, G. Raisbeck, D. Raynaud, A. Schilt, J. Schwander, E. Selmo, R. Souchez, R. Spahni, B. Stauffer, J. P. Steffensen, B. Stenni, T. F. Stocker, J. L. Tison, M. Werner, E. W. Wolff, Orbital and millennial Antarctic climate variability over the past 800,000 years. *Science* **317**, 793–796 (2007).

154. A. Berger, M.-F. Loutre, Insolation values for the climate of the last 10 million years. *Quat. Sci. Rev.* **10**, 297–317 (1991).

Citation: J. C. Thompson, D. K. Wright, S. J. Ivory, J.-H. Choi, S. Nightingale, A. Mackay, F. Schilt, E. Otárola-Castillo, J. Mercader, S. L. Forman, T. Pietsch, A. S. Cohen, J. R. Arrowsmith, M. Welling, J. Davis, B. Schiery, P. Kaliba, O. Malijani, M. W. Blome, C. A. O'Driscoll, S. M. Mentzer, C. Miller, S. Heo, J. Choi, J. Tembo, F. Mapemba, D. Simengwa, E. Gomani-Chindebvu, Early human impacts and ecosystem reorganization in southern-central Africa. *Sci. Adv.* **7**, eabf9776 (2021).

# Science Advances

## Early human impacts and ecosystem reorganization in southern-central Africa

Jessica C. Thompson, David K. Wright, Sarah J. Ivory, Jeong-Heon Choi, Sheila Nightingale, Alex Mackay, Flora Schilt, Erik Otárola-Castillo, Julio Mercader, Steven L. Forman, Timothy Pietsch, Andrew S. Cohen, J. Ramón Arrowsmith, Menno Welling, Jacob Davis, Benjamin Schiery, Potiphar Kaliba, Oris Malijani, Margaret W. Blome, Corey A. O'Driscoll, Susan M. Mentzer, Christopher Miller, Seoyoung Heo, Jungyu Choi, Joseph Tembo, Fredrick Mapemba, Davie Simengwa and Elizabeth Gomani-Chindebvu

| | |
|---|---|
| **ARTICLE TOOLS** | http://advances.sciencemag.org/content/7/19/eabf9776 |
| **SUPPLEMENTARY MATERIALS** | http://advances.sciencemag.org/content/suppl/2021/05/03/7.19.eabf9776.DC1 |
| **REFERENCES** | This article cites 125 articles, 13 of which you can access for free http://advances.sciencemag.org/content/7/19/eabf9776#BIBL |
| **PERMISSIONS** | http://www.sciencemag.org/help/reprints-and-permissions |

Use of this article is subject to the Terms of Service